Journal of Cerebral Blood Flow and Metabolism
21:782–792 © 2001 The International Society for Cerebral Blood Flow and Metabolism
Published by Lippincott Williams & Wilkins, Inc., Philadelphia

Anatomic and Biochemical Correlates of the Dopamine Transporter Ligand ^{11}C-PE2I in Normal and Parkinsonian Primates: Comparison With 6-[^{18}F]Fluoro-L-Dopa

Thomas Poyot, Françoise Condé, Marie-Claude Grégoire, *Vincent Frouin, *Christine Coulon, *Chantal Fuseau, *Françoise Hinnen, *Frédéric Dollé, Philippe Hantraye, and *Michel Bottlaender

*URA CEA CNRS 2210 and *Service Hospitalier Frédéric Joliot, Département de Recherche Médicale, Direction des Sciences du Vivant, CEA, Orsay Cedex, France*

Summary: Positron emission tomography (PET) coupled to 6-[^{18}F]Fluoro-L-Dopa (^{18}F-Dopa) remains the gold standard for assessing dysfunctionality concerning the dopaminergic nigrostriatal pathway in Parkinson's disease and related disorders. The use of ligands of the dopamine transporters (DAT) is an attractive alternative target; consequently, the current aim was to validate one of them, ^{11}C-PE2I, using a multiinjection modeling approach allowing accurate quantitation of DAT densities in the striatum. Experiments were performed in three controls, three MPTP-treated (parkinsonian) baboons, and one reserpine-treated baboon. ^{11}C-PE2I B′max values obtained with this approach were compared with ^{18}F-Dopa input rate constant values (Ki), *in vitro* Bmax binding of ^{125}I-PE2I, and the number of dopaminergic neurons in the substantia nigra estimated postmortem by stereology. In the caudate nucleus and putamen, control values for ^{11}C-PE2I B'max were 673 and 658 pmol/mL, respectively, whereas it was strongly reduced in the MPTP-treated (B′max = 26 and 36 pmol/mL) and reserpine-treated animals (B′max = 338 and 483 pmol/mL). *In vivo* ^{11}C-PE2I B′max values correlated with ^{18}F-Dopa Ki values and *in vitro* ^{125}I-PE2I Bmax values in the striatum and with the number of nigral dopaminergic neurons. Altogether, these data support the use of ^{11}C-PE2I for monitoring striatal dopaminergic disorders and the effect of potential neuroprotective strategies. **Key Words:** Baboon—Dopamine transporter—F-Dopa—MPTP—PE2I—Striatum.

Parkinson's disease (PD) is a neurodegenerative disorder mainly associated with a progressive loss of mesencephalic dopaminergic neurons and massive dopaminergic depletion within the striatum (caudate nucleus and putamen), the main target of the dopaminergic mesencephalic neurons and an area implicated in motor and cognitive behavior. Currently, no known curative therapy exists for PD. Current palliative therapies rely on drugs or surgical methods that transitorily compensate for the loss of dopamine but still fail to prevent or even slow down the disease process. Consequently, a great deal of effort is now being made to develop therapeutic interventions aimed at protecting neurons from degeneration by using neuroprotective or neurotrophic molecules, or both (Kordower et al., 2000).

In this context, quantitative *in vivo* imaging of the loss of dopaminergic cell bodies and processes would be of primordial interest as a way of monitoring the disease's progression and the potential therapeutic effects of neuroprotective treatments. Currently, positron emission tomography (PET) coupled to 6-[^{18}F] Fluoro-L-Dopa (^{18}F-Dopa) is the gold standard for studying the anatomofunctional integrity of the dopaminergic nigrostriatal pathway under the different conditions associated with dopamine dysfunction, such as PD or Parkinson-related disorders. In addition, ^{18}F-Dopa PET is used to assess the efficacy of experimental intrastriatal transplantations of fetal dopaminergic neurons in patients with PD (Rémy et al., 1995; Brundin et al., 2000). In advanced stages of PD, as well as in primate models of PD, ^{18}F-Dopa striatal uptake has been shown to correlate strictly with the number of dopaminergic neurons in the substantia nigra and

Received January 3, 2001; final revision received March 9, 2001; accepted March 12, 2001.

Supported by the Center National pour la Recherche Scientifique, the Commissariat à l'Energie Atomique, and the European Community NeuroGet grant n°. QLK3-CT-1999–00702. T. Poyot is a fellow of the French Ministry of Research and of the Fondation pour la Recherche Médicale (FDT 20000 71 0099).

Address correspondence and reprint requests to Michel Bottlaender, Service Hospitalier Frédéric Joliot, 4 place du Général Leclerc 91401 Orsay, France.

with the striatal levels of dopamine (Snow et al., 1993; Pate et al., 1993). However, in early stages of PD or after partial nigrostriatal lesions, a relative stability of dopamine (DA) striatal levels is maintained despite a noticeable cell loss in the substantia nigra, as a consequence of functional compensatory processes (Zigmond et al., 1990; Hornykiewicz, 1993; Lee et al., 2000). Moreover, it has been repetitively demonstrated that alterations in ^{18}F-Dopa striatal binding can either be interpreted as alterations in dopamine function, or in dopamine terminal density (sprouting, degeneration), or even a combination of both (Zigmond et al., 1990; Hornykiewicz, 1993; Lee et al., 2000). In addition, *in vivo* binding of ^{18}F-Dopa appears hardly quantifiable by PET in mesencephalic dopaminergic nuclei using routine procedures (Rakshi et al., 1999). Consequently, ^{18}F-Dopa cannot be used *sensus stricto* for the quantification of an alteration in dopamine cell densities, a potential powerful tool for the *in vivo* monitoring of neuroprotective strategies.

To overcome these limitations, the authors and others introduced the use of selective ligands of the dopamine transporter (DAT) as an alternative to ^{18}F-Dopa (Hantraye et al., 1992; Frost et al., 1993; Morris et al., 1996; Nurmi et al., 2000). Although ^{18}F-Dopa and DAT ligands detect dopaminergic dysfunction, the uptake of the ^{18}F-Dopa mainly reflects decarboxylation of the tracer and its storage as 6-[^{18}F]fluoro-L-dopamine in presynaptic terminals, whereas DAT uptake primarily reflects binding to presynaptic dopaminergic transporters. Therefore, ^{18}F-Dopa striatal uptake reflects both metabolic and functional indices of dopaminergic afferent striatal axons, whereas DAT ligand striatal uptake follows the density of dopaminergic axonic terminals in patients with PD. In addition, the authors' recent studies in *de novo* patients with ^{76}Br-FE-CBT strongly suggest that striatal DAT binding might be a more sensitive biomarker of disease progression than ^{18}F-Dopa, especially in the early stages of the disease (Ribeiro et al., 2000). However, few of these tracers have been extensively studied and compared with ^{18}F-Dopa (Ishikawa et al., 1996).

Searching for a better radioligand for the DAT, the authors realized the synthesis of ^{11}C-PE2I ([^{11}C]-(E)-N-(3-iodoprop2-enyl)-2β-carbomethoxy -3 β-(4′-methylphenyl) nortropane) (Dollé et al., 2000), because PE2I, a cocaine analogue, was reported to display a highly selective affinity for the DAT, both *in vitro* and *in vivo* (Emond et al., 1997; Chalon et al., 1999). Using the multiinjection paradigm for receptor-ligand binding studies developed in-house for other dopamine tracers (Delforge et al., 1991, 1999), the authors developed a quantitation of brain ^{11}C-PE2I kinetics (Bottlaender et al., 2000) allowing the determination of the apparent densities of DAT receptors (B′max) and the affinity value (KdVr) for ^{11}C-PE2I.

The goal of the current study was to validate in primates a state-of-the-art methodology that will allow *in vivo* assessment of neuroprotective therapeutics to be exploitable in future clinical trials.

MATERIALS AND METHODS

Nonhuman primates

Seven adolescent *Papio anubis* baboons (weighing 11 to 15 kg) were used in this study. Three baboons served as intact controls. Three other animals received a chronic 1-methyl-4-phenyl-1,2,3,6-tetrahydropyridine (MPTP) treatment that induces severe degeneration of mesencephalic dopaminergic neurons (Varastet et al., 1993). Finally, one animal was treated with reserpine, a dopamine-depleting agent. All animals were housed individually in standard primate cages with free access to food and water. All procedures were in strict accordance with the recommendations of the European Economic Community (86/609/EEC) and the French National Committee for the care and use of laboratory animals (87/848).

MPTP lesion

For 60 weeks, animals were treated with MPTP, administered as 1 weekly intramuscular injection. The MPTP solution (freshly prepared before each injection) was dissolved at a final concentration of 5 mg/mL in 0.9% NaCl. During the first 26 weeks, a starting dosage of 0.5 mg/kg was used and then was incremented by 0.1 mg/kg every month, finally reaching a weekly dose of 1 mg/kg for the last 14 weeks of the intoxication regimen. This chronic MPTP treatment resulted in a progressive parkinsonian syndrome that included all cardinal features of PD—hypokinesia, bradykinesia, balance impairment, postural alterations, and resting tremor. Within one month after the end of the MPTP treatment, parkinsonian animals were PET-scanned using ^{11}C-PE2I and ^{18}F-Dopa.

Reserpine treatment

In one baboon, reserpine (1 mg/kg; Sigma-Aldrich, France), dissolved in 20% ascorbic acid, was administered as a slow intravenous infusion over 20 minutes. Forty-five weeks after reserpine treatment, this animal was examined by PET at 2-week intervals using both tracers and was killed 4 weeks after the last PET examination.

Magnetic resonance imaging

Superimposition of PET images to the corresponding magnetic resonance images was used to establish with consistent precision the anatomic localization of ^{11}C-PE2I and ^{18}F-Dopa cerebral binding for each primate. For this purpose, each animal was submitted to magnetic resonance imaging (MRI) examination on a 1.5 Tesla SIGNA system (General Electric, Milwaukee, WI, U.S.A.). Animals were anesthetized by intramuscular injection of a mixture of ketamine (15 mg/kg; Ketalar, Parke-Davis, France) and xylazine (1.5 mg/kg; Rompun, Bayer, France) (Banknieder et al., 1978), and positioned into the magnet using a MR-compatible headholder. A T_1-weighted inversion-recovery sequence in three-dimensional mode and a 256 × 192 matrix over 124 slices (1.5-mm-thick) was used to generate the MR images compatible with the PET images.

Radiochemistry

^{18}F-Dopa labeling. 6-[^{18}F]fluoro-*L*-DOPA was prepared as previously described (Namavari et al., 1992; Dollé et al., 1998)

by regio-selective radiofluorodestannylation using [^{18}F]fluorine ([^{18}F]F_2, cyclotron-produced isotope, half-life = 110 minutes) and N-(formyl or *tert*-butoxycarbonyl)-3,4-di(tert-butoxycarbonyloxy)-6-trimethylstannyl-L-phenylalanine ethyl ester as the labeling precursor. Radiochemical, chemical, and enantiomerical purities of the radioligand determined by high pressure liquid chromatography (HPLC) were found to be greater than 98%, 95%, and 99%, respectively.

^{11}C-PE2I labeling. PE2I was labeled with carbon 11 (cyclotron-produced isotope, half-life = 20.4 minutes) at its methyl ester function from the corresponding carboxylic acid precursor and the highly efficient methylating reagent [^{11}C]methyl triflate. Typically, 200 to 300 mCi (7.4 to 11.1 GBq) of ^{11}C-PE2I were routinely obtained within 25 minutes of synthesis, with specific radioactivity ranging from 0.8 to 1.2 Ci/μmol (29.6 to 44.4 GBq/μmol). Radiochemical and chemical purity of ^{11}C-PE2I (determined by HPLC) was greater than 98% (Dollé et al., 2000).

Positron emission tomography

^{18}F-Dopa PET scans. ^{18}F-Dopa PET measurements were obtained with an ECAT Exact HR+ tomograph (Siemens CTI, Knoxville, TN, U.S.A.), in three-dimensional acquisition mode (63 planes, axial field of view = 155 mm, isotropic resolution = 4.5 mm full width at half maximum) (Adam et al., 1997). The scatter correction was calculated using the Klein–Nishma formulae, a map of scattered coincidences from the map of attenuation (Watson et al. 1997). In the reconstructed images (Hanning apodizing window), the final spatial resolution was 6.8 mm.

Anesthetized animals (ketamine:xylazine mixture, 15:1.5 mg/kg) were positioned in the PET tomograph, with their head held in a fixed position, using the same head holder as for MRI. A 15-minute transmission scan was first performed using ^{68}Ge sources to correct for γ-ray attenuation. ^{18}F-Dopa (148 MBq on average, in 10 mL of 0.9% NaCl) was then injected intravenously over 60 seconds. The ^{18}F-Dopa scanning protocol included 9 frames of 10 minutes each, starting immediately after the tracer injection. Positron emission tomography and MR images were coregistered using a rigid body matching algorithm that maximizes a mutual information criterion (Maes et al., 1997). Regions of interest (ROIs) covering the caudate nucleus, putamen, midbrain mesencephalic dopaminergic nuclei, and cerebellum were manually defined on registered images and then copied onto corresponding PET images. Radioactive concentrations in the different ROIs then were calculated for each sequential PET scan and plotted versus time. ^{18}F-Dopa uptake rate constants (Ki values) were determined in caudate and putamen using the multiple-time graphic analysis (Patlak and Blasberg, 1985).

^{11}C-PE2I PET scans. ^{11}C-PE2I PET studies were performed with an ECAT 953B/31 tomograph (Siemens CTI), in two-dimensional acquisition mode, allowing simultaneous reconstruction of 31 slices every 3.3 mm with intrinsic spatial and axial resolutions of 5.7 mm and 5.0 mm, respectively (Bendriem, 1991). In the reconstructed images (Hanning apodizing window), the spatial resolution was 8.8 mm. Animals were anesthetized with a mixture of isoflurane/nitrous oxide (1%/66%) with 33% oxygen, monitored using an Ohmeda ventilator (OAV 7710; Ohmeda, Madison, WI, U.S.A.). The tidal volume was adjusted to achieve stable end-tidal carbon dioxide tension between 38 to 40 mm Hg. Positioning of the baboon in the PET scanner and γ-ray attenuation was performed as described above for ^{18}F-Dopa scans. *In vivo* ^{11}C-PE2I binding kinetics were quantified using a multiinjection modeling approach (Delforge et al., 1991, 1999). Forty-eight sequential PET scans were acquired with image acquisition times varying from 15 seconds to 5 minutes. The experimental protocol consisted of three consecutive injections of labeled and/or unlabeled ligand. This protocol allows the evaluation, from a single experiment, of both the apparent concentration of dopamine transporter sites (B′max) and the equilibrium dissociation constant (Kd), within selected ROIs and only requires one synthesis of ^{11}C-PE2I (Bottlaender et al., 2000). At the beginning of the experiment (T0), one injection of the labeled compound (range 3.8 to 24.1 nmol) was performed. At time T0 + 40 minutes, a second intravenous injection was performed, consisting of a mixture of labeled (range 32 to 120 nmol) and unlabeled PE2I in the same syringe. The amount of unlabeled compound injected was calculated to achieve a partial (approximately 50%) saturation of the dopamine transporter sites *in vivo*. As shown in Table 1, the dose of unlabeled compound injected varied from 1476 to 2156 nmol in normal or reserpine-treated animals to 46 to 338 nmol in MPTP-lesioned animals. At time T0 + 80 minutes, a third injection consisting of a large excess of unlabeled PE2I (3432 to 8011 nmol) was performed. As the plasma time-concentration curve was used to establish the input function in the model, 69 arterial blood samples were collected from the femoral artery (Fig. 1). Given that the fraction of nonmetabolized ^{11}C-PE2I decreased rapidly after the intravenous administration (inset in Fig. 1), the authors used the metabolite-corrected plasma curve as the final input function in the model. To this aim, the amount of unchanged radiotracer in plasma was measured in selected samples (5 for each of the 3 injections) to correct the ^{11}C-PE2I plasma time-concentration curve for peripheral metabolism. The total experiment was 130 minutes in duration. Details of the doses administered and specific activity at time T0 are given in Table 1. The modeling approach for ^{11}C-PE2I is based on a 4-compartment ligand-receptor model involving 7 parameters (B′max, KdVr, and 5 different kinetic parameters), as previously described (Bottlaender et al., 2000). The authors have shown previously that PE2I major metabolites are polar and do not enter the brain.

Regions of interest were defined on MR images and copied onto the corresponding PET images. Radioactivity was measured in each selected ROI, corrected for ^{11}C decay, and expressed as pmol/mL of tissue, taking into account the corresponding specific radioactivity of the radiotracer measured at time T0. After rapid blood centrifugation, plasma [^{11}C] radioactivity was measured using a γ-counter (Cobra, Packard, France) and the time-activity curves were corrected for [^{11}C] decay from the time of the corresponding injection.

Postmortem studies

All animals were killed with a lethal dose of pentobarbital (100 mg/kg, intravenously; Sanofi, France). Immediately after

TABLE 1. *Labeled and unlabeled PE2I injected doses and radiotracer specific activity at time T0*

			T0 + 40 minutes		T0 + 80 minutes unlabeled (nmol)
	Sp. activity (mCi/mmol)	To minutes tracer (nmol)	Tracer (nmol)	Unlabeled (nmol)	
Control 1	512	9.2	51	1476	7128
Control 2	822	7.6	34.6	1630	7684
Control 3	493	3.8	32	2007	8011
MPTP 1	234	24.1	120	338	3432
MPTP 2	612	6.9	58	184	6415
MPTP 3	284	14.9	48	46	5093
Reserpine	494	9.8	55	2156	0

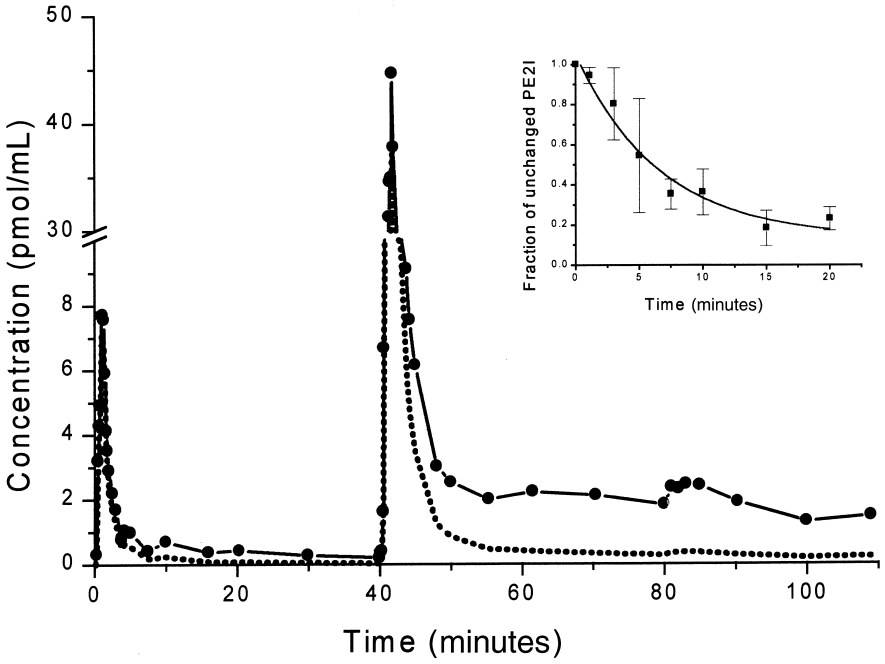

FIG. 1. Arterial plasma time-activity curve of ^{11}C-PE2I (solid line and symbols) as measured in a multiinjection study. The dotted line represents the metabolite-corrected plasma curve used as input function in the model. Data are from the second experiment in one control animal. (Inset) Fraction of unchanged PE2I in the plasma (mean ± SD of the seven experiments).

death, the brain was removed from the skull, and the two hemispheres were separated and cut into coronal blocks (5- to 10-mm-thick). Blocks from one hemisphere were immersed in isopentane at −80°C and stored at −80°C. Blocks from the other hemisphere were immersed for 5 days in PLP (paraformaldehyde 2%, sodium m-periodate 0.20%, L-lysine monohydrochloride 1.4% in 0.1 mol/L phosphate buffer) at 4°C. They then were immersed in a graded series of sucrose phosphate-buffered solutions (12%, 16%, and 18%). Coronal sections (40-μm-thick) were cut with a freezing microtome (Microm, Francheville, France), kept in anatomic series in a cryoprotective solution (glycerol and ethylene glycol 30% in 0.1 mol/L phosphate buffer), and stored at −20°C until further processing.

Histology. The presence of catecholaminergic neurons was revealed by tyrosine hydroxylase (TH) immunocytochemistry. Free-floating sections were incubated for 30 minutes at room temperature in phosphate-buffered saline (PBS; pH 7.4) containing 0.3% Triton-X 100 (TX-100) and 5% normal goat serum. Sections then were incubated for 48 hours at room temperature or 72 hours at 4°C in PBS containing 0.3% TX-100, 3.5% normal goat serum, 0.05% bovine serum albumin, and a rabbit anti-TH antiserum (Institut Jacques Boy, France) diluted 1:10,000. Sections then were processed by the avidin-biotin peroxidase method of Hsu et al. (1981), using Vectastain and VIP kits (Vector Laboratories, U.S.A.).

Stereologic analysis. Quantitative analyses of the number of TH-immunoreactive neurons in the substantia nigra were performed on a computer-assisted image analysis system consisting of an Olympus Provis microscope (Olympus France, Rungis, France) with a computer-controlled motorized stage, a Sony HAD Power 3CCD video camera, an Olympus Pentium II computer, and C.A.S.T.-Grid (Olympus Denmark, Albertslund, Denmark), the Olympus stereology software. Stereologic analyses were performed using the optical fractionator (West et al., 1991, 1996). By using a random starting point, a 1:10 series of sections was sampled throughout the entire substantia nigra (yielding 20 to 25 sections per animal, depending on the case). After outlining the boundaries of the substantia nigra on the computer graphic display in each section separately, the C.A.S.T.-grid software placed within each boundary a set of optical dissector frames (100 × 100 μm) in a systematic, randomized fashion, corresponding to a predetermined percentage of the sampled area that was kept constant throughout the study (35%). TH-positive neurons then were counted in each stack of optical dissectors (each dissector was 1 μm in depth), according to stereologic principles. The thickness of these dissector stacks was kept constant within each animal and was set at 8 μm in the current study. All analyses were performed using a ×60 Plan-Neofluar objective. The total number of TH-positive neurons in the substantia nigra was then obtained by the using the formula developed by West et al. (1991): $N = \Sigma Q^{-}$. 1/asf · 1/ssf · 1/tsf, where the number of neurons (N) is defined by the total number of neurons ΣQ^{-} counted in the dissectors located within the defined subdivisions of the sampled sections, multiplied by the area, section, and thickness sampling fractions (asf, ssf, and tsf, respectively).

***In vitro* binding assay.** *In vitro* binding assays were performed on caudate nucleus and putamen membranes from the left brain hemisphere. Brain tissues were homogenized with a Dounce apparatus in 10 volumes of ice-cold sucrose (0.32 mol/L). The tissue homogenate was first centrifuged for 10 minutes at 1,000 *g*. The pellet then was suspended in sucrose and centrifuged a second time. The two supernatants were collected and centrifuged again for 30 minutes at 17,500 *g* at 4°C. The pellets then were suspended in 20 volumes of incubation buffer (TRIS 50 mmol/L, NaCl 120 mmol/L, KCl 5 mmol/L, pH 7.4) and centrifuged for 10 minutes at 50,000 *g* at 4°C. The pellets then were resuspended in a minimum volume of incubation buffer. Protein content was determined according to the method of Lowry (Lowry et al., 1951). For saturation analysis, assays were run in triplicate with increasing concentrations of ^{125}I-PE2I (kindly provided by Cis-Bio International, France) ranging from 0.3 to 40 nmol/L in 1 mL of TRIS buffer to obtain a final protein concentration of 30 μg/mL. Nonspecific binding was determined using a large excess of cocaine (30 μmol/L), a competitive inhibitor of PE2I. Samples were incubated at 22°C for 1.5 hours, then filtered under reduced pressure on glass fiber filters (Whatman GF/C) using a cell harvester system

(EEG-Instrument, Evry, France). Filters were washed with ice-cold TRIS-HCl buffer (50 mmol/L, pH 7.4), and the radioactivity remaining on the filters was measured in a well γ-counter (Cobra, Packard, France). Kd and B′max binding parameters then were calculated using an iterative nonlinear least square curve fitting program (GraphPad Prism®, San Diego, CA, U.S.A.).

RESULTS

^{11}C-PE2I PET studies

The superimposition of PET images to the corresponding MR images showed that ^{11}C-PE2I binding in control primates (Fig. 2) and in the reserpine-treated animal was mostly restricted to striatal regions, namely the caudate nucleus and the putamen. In addition, an activity concentration was visualized in the ventral midbrain (Fig. 2, arrows), in an area corresponding to the substantia nigra and the ventral tegmental area. Low activity levels were measured in other brain regions, notably in the cerebellum and the cerebral cortex. In the MPTP-treated animals, the nonsupervised MRI/PET coregistration could not be obtained because of technical problems on MR image acquisition. The MRI-PET coregistration was performed manually, which has proven to give similar results (Pietrzyk et al., 1994).

Figure 3 shows representative examples of time-concentration curves obtained in one control (Fig. 3A) and one MPTP-treated baboon (Fig. 3B), with the multiinjection protocol. These curves correspond to the kinetics of ^{11}C-PE2I obtained in the caudate nucleus, putamen, midbrain, and cerebellum of the "Ctrl3" and "MPTP2" animals described in Table 2. In the control baboon (Fig. 3A), caudate and putamen uptake reached a plateau within 10 minutes after the first injection of labeled ligand and remained stable until the second injection, except in the midbrain and cerebellum where an appreciable washout was observed. After the second injection of labeled and unlabeled ligand, ^{11}C-PE2I uptake peaked within 4 to 5 minutes and was followed by an appreciable washout in the caudate and putamen, and, to a greater extent, in the midbrain and the cerebellum. The last injection of unlabeled ligand produced a further displacement of the ^{11}C-PE2I binding in both striatal regions and to a lesser extent in the midbrain, whereas the cerebellar kinetics were unaffected. Activity ratios between transporter-rich regions and cerebellum were high (for example, 7.06 ± 0.47 and 7.63 ± 0.47 during the 30- to 40-minute interval, and 3.38 ± 0.17 and 3.21 ± 0.14 during the 70- to 80-minute interval in caudate and putamen, respectively).

In the striatum of the MPTP-treated monkeys (Fig. 3 B), ^{11}C-PE2I kinetics were roughly similar to those observed in the cerebellum. However, a marked decrease in the uptake peak was observed after the second injection and the displacement in the caudate and putamen was further reduced after the third injection. Activity ratios between transporter-rich regions (caudate, putamen, and midbrain) and cerebellum were less in the MPTP-lesioned animals (for example, 2.64 ± 0.17 and 2.71 ±

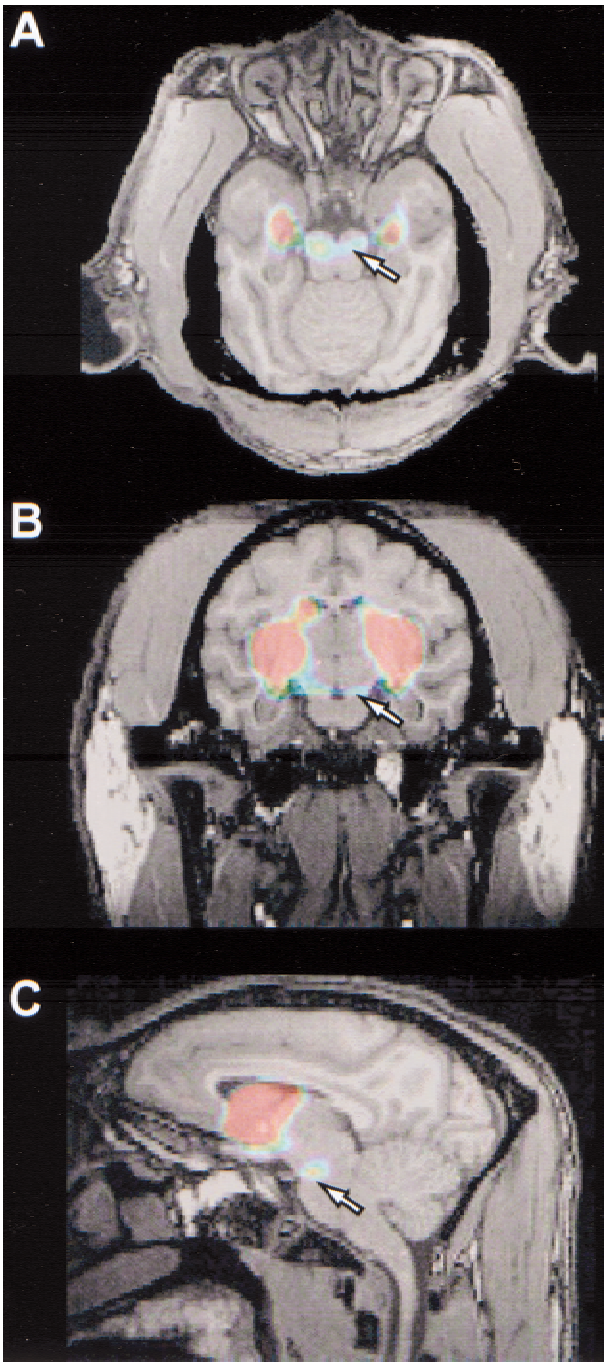

FIG. 2. ^{11}C-PE2I tomographic images superimposed on corresponding magnetic resonance images in one control baboon ("Ctrl1" in Table 2) in axial **(A)**, coronal **(B)**, and sagittal **(C)** views. A high specific ^{11}C-PE2I binding (red, yellow) can be easily detected in the DAT-enriched striatal regions (caudate nucleus, putamen). A moderate binding (yellow, blue) can also be identified in the ventral midbrain region (arrows in **A**, **B**, and **C**), corresponding to the anatomic localization of the substantia nigra and ventral tegmental area.

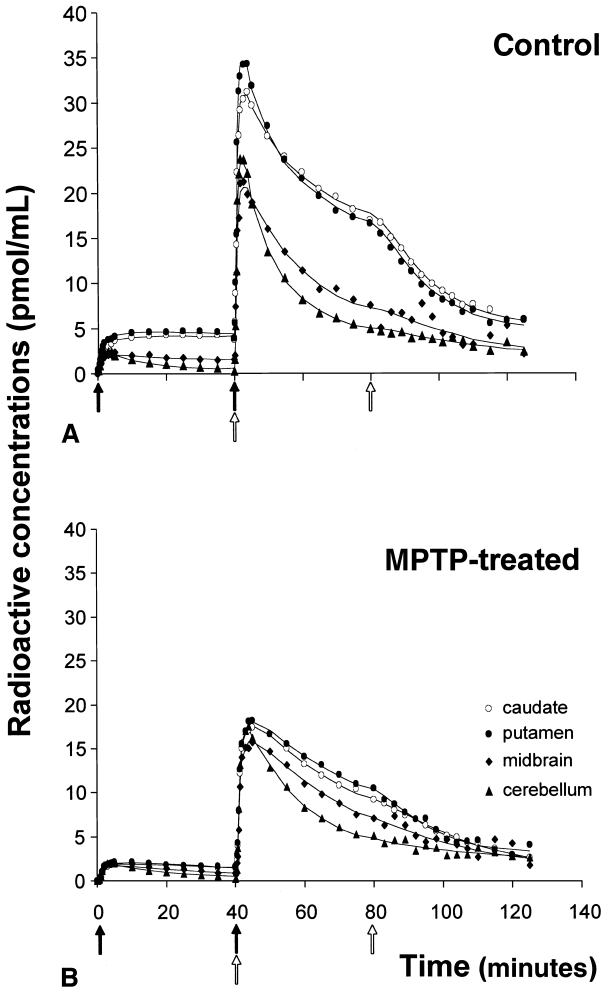

FIG. 3. Representative PE2I time-activity curves obtained from one control **(A)** and one MPTP-treated baboon **(B)**. Solid lines correspond to the best fitted curve for data recorded in each of the different regions of interest (o, caudate nucleus; ●, putamen; ♦, midbrain; ▲, cerebellum). Arrows point to the times of intravenous injections of the various labeled (⟶) and unlabeled (⟹) PE2I dosages (see Table 1 for details).

0.15 during the 30 to 40 minutes, and 1.89 ± 0.06 and 2.09 ± 0.08 during the 70- to 80-minute intervals in caudate and putamen, respectively).

In vivo estimates of ^{11}C-PE2I binding parameters by the multiple-injection modeling approach are summarized in Table 2. As PET image intensities measured in the midbrain were greatly influenced by the partial volume effect introduced by the small size of this structure in the nonhuman primate relative to the spatial resolution of the tomograph used, midbrain kinetics were not analyzed using the multiple-injection modeling approach. However, in the case of the caudate and putamen kinetics, the 4-compartment model allowed the correct identification of all parameters, including the apparent transporter density (B′max) and affinity (KdVr) in all animals, even in the 2 most severely MPTP-lesioned baboons. In control baboons, caudate and putamen B′max values were 674 ± 71 and 658 ± 103 pmol/mL, respectively. In the same regions, calculated KdVr values were 33.3 ± 17.6 and 25.1 ± 11.1 nmol/L, respectively. Sixty weeks of chronic MPTP treatment induced a marked decrease in B′max values within the striatum (26.3 ± 20.9 and 36.0 ± 29.7 pmol/mL in caudate and putamen, respectively), whereas KdVr value changes were not statistically significant (24.0 ± 12.3 and 56.6 ± 47.0 nmol/L). These alterations represented an average decrease of 96% in the caudate nucleus and 95% in the putamen. In the caudate and putamen of the only animal treated with reserpine, marked decreases in ^{11}C-PE2I binding density were found (338 and 483 pmol/mL corresponding to 31% and 29% decrease compared with controls), whereas KdVr values remained in the normal range.

^{18}F-Dopa PET studies

As summarized in Table 2, average Ki values calculated in the caudate and putamen of control animals were $6.9 \pm 1.2 \times 10^{-3}$ and $7.7 \pm 1.8 \times 10^{-3}$ min^{-1}, respectively. In MPTP-treated animals, highly significant 90% and 95% reductions of these Ki values were observed in the caudate ($1.1 \pm 1.0 \times 10^{-3}$ min^{-1}) and putamen ($0.6 \pm 0.6 \times 10^{-3}$ min^{-1}), respectively. In the animal treated with reserpine, no significant changes in Ki values were noted in the caudate or putamen compared with controls.

Postmortem data

^{125}I-PE2I binding assay. As shown in Table 2, the specific binding of ^{125}I-PE2I was studied in the caudate nucleus and putamen of all animals but one (Ctrl3), in which brain homogenates could not be processed properly. In the control animals, average Bmax values in caudate and putamen were 203 and 249 pmol/g, respectively. In the caudate and putamen of the MPTP-treated animals, the marked loss in specific binding observed *in vivo* was confirmed *in vitro*. Bmax values determined in the caudate and putamen of these severely parkinsonian animals were 24.7 ± 12.7 and 18.2 ± 10.6 pmol/g tissue, respectively, representing a 87.7% and 92.7% decrease compared with control animals. In the animal treated with reserpine, a trend decrease in Bmax values was also observed in both striatal regions (30% and 27% decreases in caudate and putamen respectively) compared with control animals, which was in agreement with *in vivo* B′max values.

Tyrosine hydroxylase immunocytochemistry and stereologic cell counts

In control and reserpine-treated animals, there was a dense TH immunoreactivity throughout the striatum (Fig. 4A and 4E), whereas in the MPTP-treated animals,

TABLE 2. In vivo *PET data,* in vitro *^{125}PE2I binding parameters and stereologic neuronal counts in control, MPTP-and reserpine-treated baboons*

		In vivo PET data			Postmortem parameters		
		^{11}C-PE2I		^{18}F-Dopa	^{125}I-PE2I *in vitro* binding		Stereologic counts
Animals	Brain region	B′ max (pmol/mL)	KdVr (nmol/L)	Ki (10^{-3} min^{-1})	Bmax (pmol/g)	Kd (nmol/L)	Number of TH-immunoreactive neurons in the substantia nigra
Control 1	Cd	637	19.1	7.4	264	3.28	217572
	Put	765	15	9.5	275	2.83	
Control 2	Cd	628	27.8	5.5	143	3.85	166158
	Put	560	23.3	5.9	224	2.99	
Control 3	Cd	756	53	7.7	ND	ND	201805
	Put	650	37	7.6	ND	ND	
Mean (SD)	Cd	673.6 (71.4)	33.3 (17.6)	6.9 (1.2)	203.5 (85.6)	3.56 (0.40)	195178 (26339)
Mean (SD)	Put	658.3 (102.7)	25.1 (11.1)	7.7 (1.8)	249.5 (36.1)	2.91 (0.11)	
MPTP 1	Cd	50	38	1.8	15	4.09	49660
	Put	70	103.8	1	19.5	6.16	
MPTP 2	Cd	19	19.1	1.5	39	10.71	96376
	Put	23	9.9	0.9	7	1.67	
MPTP 3	Cd	10	14.9	0.01	20	14	54385
	Put	15	56	0.01	28	19.5	
Mean (SD)	Cd	26.3 (20.9)	24.0 (12.3)	1.1 (1.0)	24.7 (12.7)	9.59 (5.0)	66807 (25716)
Mean (SD)	Put	36.0 (29.7)	56.6 (47.0)	0.6 (0.6)	18.2 (10.6)	9.11 (9.2)	
Reserpine	Cd	338	31.8	7.1	140	2.63	173486
	Put	483	45.4	8.4	178	2.65	

Cd, caudate; Put, putamen; ND, not determined.

the TH immunoreactivity in the caudate (Fig. 4C) and putamen nuclei was patchy with areas nearly devoid of any immunoreactive processes and areas containing thick, strongly immunoreactive fibers with sprouting-like branching (Song and Haber, 2000). A gradient of density was observed, the lateral part of the caudate nucleus and putamen being more depleted than its medial part. In the substantia nigra, TH immunoreactivity was not different between the reserpine-treated animal (Fig. 4F) and the controls (Fig. 4B), whereas a strong loss of TH-immunoreactive cell bodies and processes was observed in MPTP-treated animals (Fig. 4D). Quantitatively (Table 2), MPTP induced a 66% decrease ($P < 0.001$) in the number of TH-immunoreactive neurons in the substantia nigra compared with intact animals (195,178 ± 26,339 TH-immunoreactive neurons in control vs. 66,807 ± 25,716 in MPTP-treated baboons). In the reserpine-treated animal, the number of TH-immunoreactive neurons in the substantia nigra was not different from controls (Table 2).

Correlations among *in vivo* PET data, postmortem cell counts, and ^{125}I-PE2I binding parameters

The ^{11}C-PE2I binding parameter B′max determined *in vivo* by the multiple-injection modeling approach strictly correlated with ^{125}I-PE2I Bmax determined *in vitro* in putamen (Fig. 5A; $r^2 = 0.99$, $P < 0.0001$) and caudate ($r^2 = 0.98$, $P < 0.0001$) membranes; the intercept was not different from zero in both cases. ^{11}C-PE2I B′max values also strictly correlated with striatal ^{18}F-Dopa Ki values in the putamen (Fig. 5B; $r^2 = 0.93$, $P < 0.0001$) and caudate ($r^2 = 0.83$, $P < 0.005$); the intercept was also not different from zero in both cases. The estimate number of TH-immunoreactive neurons present in the substantia nigra correlated significantly with the B′max values of ^{11}C-PE2I determined by PET in putamen (Fig. 5C; $r^2 = 0.96$, $P < 0.0001$) and caudate ($r^2 = 0.86$, $P < 0.003$, not shown), with ^{125}I-PE2I *in vitro* binding values ($r^2 = 0.92$, $P < 0.005$, and $r^2 = 0.87$, $P < 0.01$, respectively), and with ^{18}F-Dopa Ki values in the putamen and caudate nucleus ($r^2 = 0.93$ and 0.96, $P < 0.0004$ and 0.0001, respectively), with an intercept at approximately 50.000 neurons for all 3 correlations.

DISCUSSION

Several compounds have been proposed to characterize the regional DAT distribution as well as its physiology and pharmacology *in vitro* and *in vivo*. The cocaine analogues, such as β-CFT (WIN-35,428), [^{123}I]β-CIT, [^{11}C]β-CIT, or more recently β-CIT-FE and β-CIT-FP, have been shown to be suitable tracers for *in vivo* studies with PET or single photon emission computed tomography (Canfield et al., 1990; Hantraye et al., 1992; Frost et al., 1993; Neumeyer et al., 1994). The authors selected a new tropane analogue, the PE2I, because of its greater *in vitro* and *in vivo* specificity for the dopamine transporter (Chalon et al., 1999). Compared with other tropane analogues that have a significant affinity for the serotonin (5HT) transporter, PE2I is much more selective. Indeed, PE2I displays a 29× and 60× greater affinity for the DAT

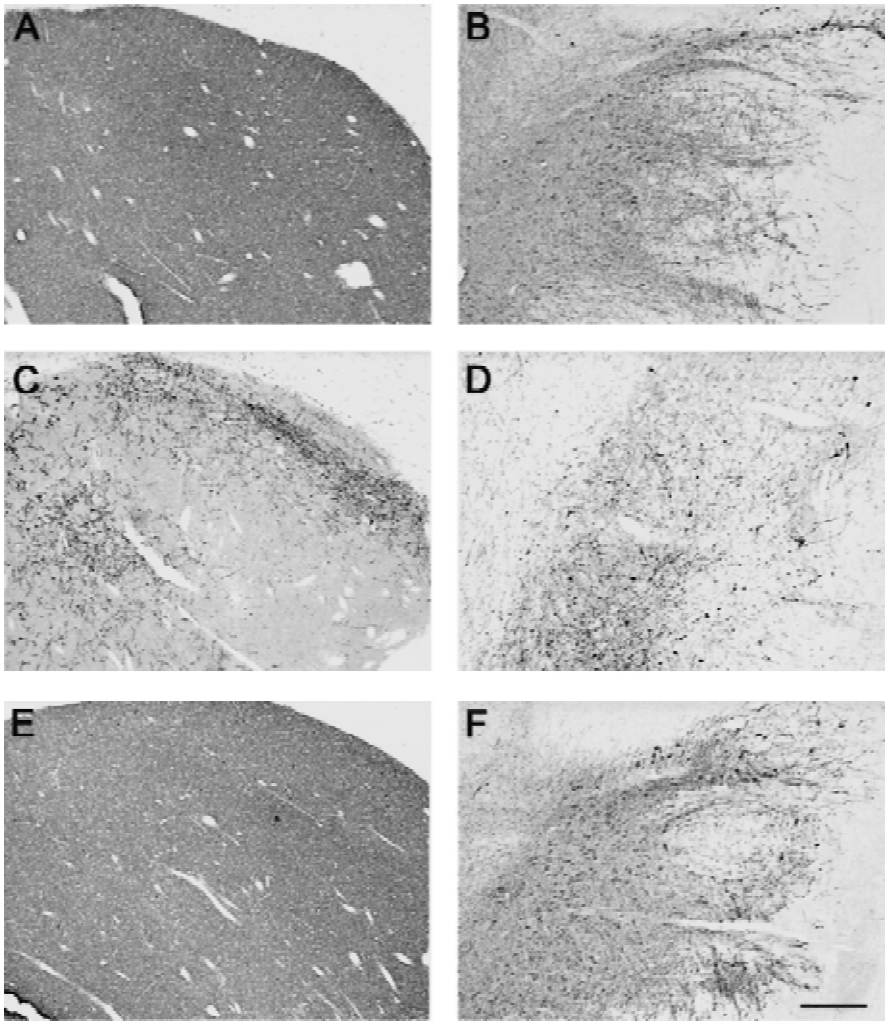

FIG. 4. Bright field photomicrographs of coronal brain sections through the lateral caudate nucleus **(A, C, E)** and lateral substantia nigra **(B, D, F)**, immunostained for tyrosine hydroxylase, from one control **(A** and **B)**, one MPTP-treated **(C** and **D)**, and the reserpine-treated animal **(E** and **F)**. In the MPTP-treated animal, note the marked decrease in the number of TH-immunoreactive neurons in the substantia nigra **(D)**, associated with the corresponding depletion in TH-immunoreactive processes in the caudate nucleus **(C)**, compared with the control **(A** and **B)** and the reserpine-treated baboon **(E** and **F)**. Scale bar = 500 μm.

than for the 5HT-transporter and the noradrenaline transporter, respectively (Emond et al., 1997). In the context of PD, this property may be important as it is known that this disorder not only affects dopamine neurons but also other monoaminergic neurons, although to a lesser extent. In fact, in MPTP-treated primates, the progressive decrease in the number of dopaminergic processes is associated with a progressive increase in the number of serotoninergic processes (Gaspar et al., 1993). Therefore, the greater selectivity of ^{11}C-PE2I for the DAT would allow more specific studies of the effects of PD on striatal dopaminergic axonal endings, independently of the possible compensatory sprouting of the 5HT axons.

Another interest of ^{11}C-PE2I resides in its high signal-to-noise ratio that allowed the authors to image *in vivo* not only the areas expressing a high density in DAT (caudate and putamen) but also the ventral portion of the midbrain, a region expressing an intermediate density of DAT but containing the dopaminergic neurons of the substantia nigra and ventral tegmental area that project to the striatum (Kaufman et al., 1991). Even in the relatively small primate brain, the precise localization of this ^{11}C-PE2I binding to the ventral midbrain was made possible by the use of a new dedicated software that superimposes in three dimensions the MRI of each individual baboon with the corresponding PET images. However, despite precise registration with the substantia nigra and ventral tegmental area, an accurate quantitation of B′max could not be achieved in this area, largely because of the small size of this region compared with the resolution of the tomograph that was used. It is likely that new methods specifically designed for correction of partial volume effects will be required before actually quantifying DAT binding in the ventral mesencephalon of humans and nonhuman primates.

To quantify ^{11}C-PE2I binding, the authors used a multiple-injection modeling approach that has already been successfully used for the absolute *in vivo* quantification of dopaminergic and nondopaminergic receptor binding in nonhuman primates (Delforge et al., 1991, 1993, 1999). This method is interesting because it does not require any reference to an appropriate region for

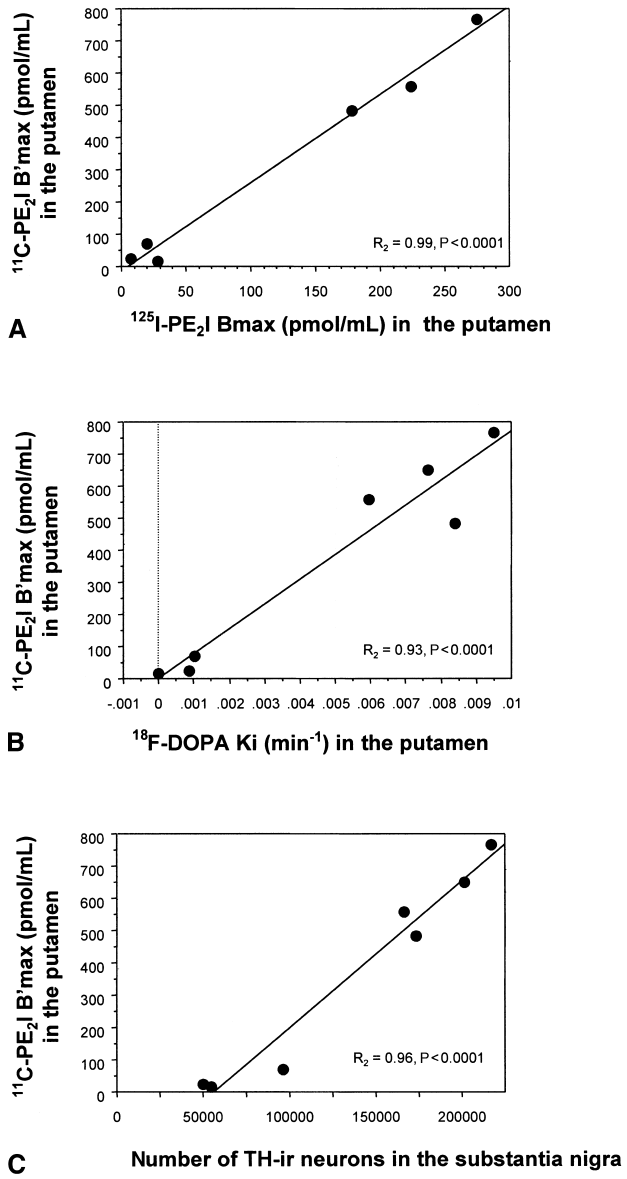

FIG. 5. Correlations between *in vivo* ^{11}C-PE2I binding parameters in the putamen and *in vitro* ^{125}I-PE2I Bmax **(A)**, ^{18}F-Dopa influx rate constant **(B)**, and the number of TH-immunoreactive (TH-ir) neurons in the substantia nigra **(C)**. Solid lines represent the best fit for regression lines. Note that in **C** the regression line does not pass through the origin (intercept at approximately 50,000 neurons), whereas regression lines for **A** and **B** do pass through the origin (strict positive correlation).

estimating the *in vivo* nonspecific binding of the tracer and also provides improved estimates of transporter number and affinity, separately. The full experimental protocol used for ^{11}C-PE2I in the current study cannot be used for human studies, but a simplified protocol is being designed, as previously performed with other PET ligands (Delforge et al., 1996).

A consistent finding of the current study was the 50% difference between B′max values observed *in vivo* and *in vitro* in the very same animals. A similar discrepancy between *in vivo* and *in vitro* results has already been reported in MPTP-treated monkeys (Pate et al., 1993) and in humans (Snow et al., 1993); it can be attributed to methodological differences and needs further studies. However, the authors observed a strong correlation (with a zero intercept) between *in vivo* values of striatal ^{11}C-PE2I B′max and *in vitro* striatal ^{125}I-PE2I Bmax. A similar, highly significant correlation was found in the caudate and putamen, regardless of the animal's condition (control, MPTP-, or reserpine-treated). This suggests that *in vivo* ^{11}C-PE2I B′max values can be used in the striatum as a measure of the total number of DAT under different physiologic or pathologic conditions. Interestingly, there was also a strong correlation between *in vivo*

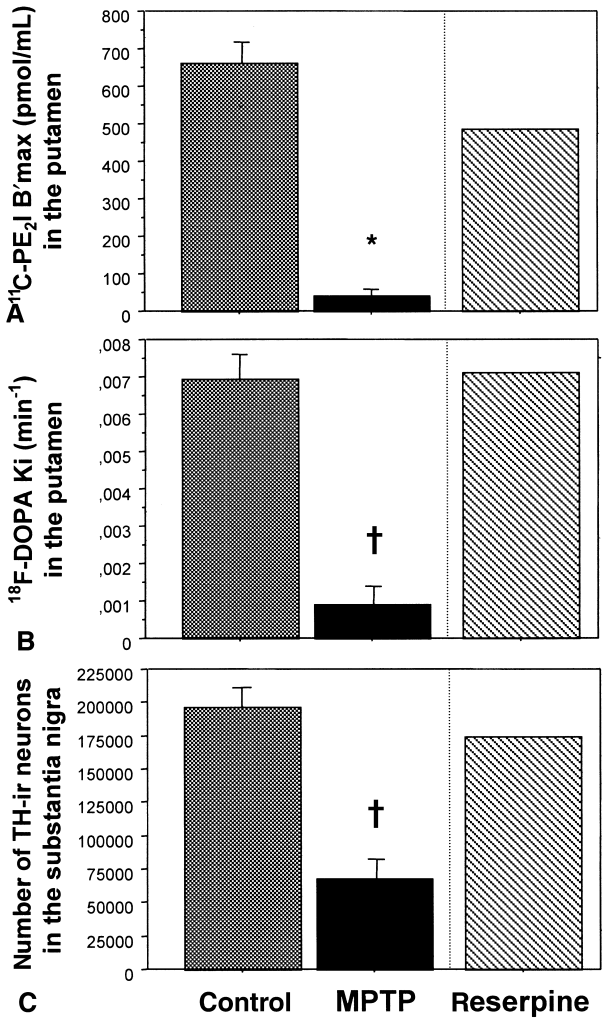

FIG. 6. (A) *in vivo* ^{11}C-PE2I B′max, **(B)** *in vivo* ^{18}F-Dopa Ki values in the putamen, and **(C)** number of TH-immunoreactive neurons in the substantia nigra of control, MPTP-treated, and reserpine-treated animals. Note the severe decrease of all dopamine markers in the MPTP-treated animals. In contrast, whereas both *in vivo* and *in vitro* PE2I binding values were decreased in the reserpine-treated animal, no significant changes were noted in putamen ^{18}F-Dopa Ki values. *P < 0.0001 versus controls; †P < 0.005 versus controls.

^{11}C-PE2I B′max values in the caudate or putamen and the total number of TH-immunoreactive neurons in the substantia nigra. Although ^{11}C-PE2I *in vivo* binding estimates were correlated with the number of nigral TH-immunoreactive neurons, the best-fit line does not pass through the origin but crosses the x-axis for approximately 50,000 neurons (Fig. 5C). This could suggest that the striatal innervation originating from 50,000 TH-immunoreactive neurons located in the substantia nigra might not induce a signal strong enough to be detected by PET in the striatum. Nevertheless, the best-fit line of the correlation between ^{125}I-PE2I *in vitro* binding and the number of nigral TH-immunoreactive neurons crosses the x-axis at the same value, that is, approximately 50,000 neurons. Therefore, it seems more likely that the chronic MPTP treatment has induced a loss of dopaminergic axon terminals or adaptative changes in presynaptic dopaminergic terminals such as down-regulation of the DAT binding sites to increase the synaptic dopaminergic concentration. A decrease in DAT binding because of antiparkinsonian medications (Kilbourn et al., 1992) can be ruled out in the three MPTP-treated animals as none of them received any treatment during the entire course of the study.

As ^{18}F-Dopa and ^{11}C-PE2I measure different aspects of the dopaminergic function, the combined use of these tracers in the same PET study may help to detect possible compensatory mechanisms in the dopamine-depleted striatum. This may be of major interest to monitor the effect of the different compounds used as neurotrophic or neuroprotective agents for PD. In the current study, ^{11}C-PE2I B′max values were correlated with ^{18}F-Dopa Ki values obtained in the caudate or putamen of control and MPTP-treated animals. For MPTP-treated animals, this finding implies that most of the decrease observed in the striatal ^{18}F-Dopa uptake is related to a loss of dopaminergic presynaptic terminals and that no increase in ^{18}F-Dopa striatal uptake occurs in these severely lesioned animals as a compensatory response to the dopamine depletion. This contrasts with recent findings in patients with PD (Lee et al., 2000) and with data from other animal models of PD in which an increased turnover of dopamine has been consistently observed in residual dopaminergic neurons, following extensive degeneration of the nigrostriatal pathway (Zigmond et al., 1990). The MPTP-treated baboons of the current study displayed a severe loss of dopaminergic processes as reflected by their clinical status, tyrosine-hydroxylase immunocytochemistry, and *in vitro* ^{125}I-PE2I binding. It is possible that after a large striatal deafferentation, the PET signal derived from the remaining striatal dopaminergic terminals may decrease below the limits of the spatial resolution of the PET scan, which in turn could induce an underestimation of the actual striatal radioactive concentrations. In line with this, the case of the one animal treated with reserpine is exemplary. As demonstrated postmortem, this animal presented a reduction in the ^{125}I-PE2I binding in the putamen and caudate (Table 2, decreases of 30% and 27% vs. controls, respectively), with no significant changes in the number of TH-immunoreactive neurons in the substantia nigra (Table 2) or in the TH immunoreactivity of the striatum (Fig. 4E). Interestingly, in the striatum of this animal, the *in vivo* ^{11}C-PE2I binding was depleted (Fig. 6A) to a similar extent (31% and 29%) as *in vitro*, whereas no significant alteration was observed in the *in vivo* ^{18}F-Dopa uptake in the striatum (Fig. 6B) or in the number of nigral TH-immunoreactive neurons (Fig. 6C). These data suggest a long-lasting down-regulation of the DAT induced by reserpine (Vilpoux et al., 2000) without changes in dopamine function. This result further illustrates the interest of combining various PET tracers to study pathologic conditions associated with acute or chronic dopamine dysfunction.

In conclusion, the current results show that PE2I can be used to estimate directly from PET data the density of DAT sites in the striatum of primates. With a simplified modeling protocol, which is being developed in-house, PE2I may become an alternative and complementary tool to ^{18}F-Dopa for monitoring PD progression and the potential benefits of new therapeutic interventions.

Acknowledgments: The authors thank C. Jouy and F. Sergent for their help and outstanding care of the primate colony and J.-M. Hermel for his excellent photographic assistance.

REFERENCES

Adam LE, Zaers J, Ostertag H, Trojan H, Belleman ME, Brix G (1997) Performance evaluation of the whole-body PET scanner ECAT EXACT HR+ following the IEC standard. *IEE Trans Nucl Sci* 44:1172–1179

Banknieder AR, Phillips JM, Jackson KT, Vinal SI Jr (1978) Comparison of ketamine with the combination of ketamine and xylazine for effective anesthesia in the rhesus monkey (Macaca mulatta). *Lab Anim Sci* 28:742–745

Bendriem B (1991) Quantitative evaluation of a new brain tomograph the ECAT 953B/31. *J Nucl Med* 32:1063

Bottlaender M, Valette H, Dollé F, Emond P, Fuseau C, Coulon C, Demphel S, Guilloteau D, Delforge J (2000) *In vivo* quantification by PET of the dopamine transporters (DAT) using the multi-injection approach and [^{11}C]PE2I [abstract]. *J Nucl Med* 41:208

Brundin P, Pogarell O, Hagell P, Piccini P, Widner H, Schrag A, Kupsch A, Crabb L, Odin P, Gustavii B, Björklund A, Brooks DJ, Marsden CD, Oertel WH, Quinn NP, Rehncrona S, Lindvall O (2000) Bilateral caudate and putamen grafts of embryonic mesencephalic tissue treated with lazaroids in Parkinson's disease. *Brain* 123:1380–1390

Canfield DR, Spealman RD, Kaufman MJ, Madras BK (1990) Autoradiographic localization of cocaine binding sites by [3H]CFT ([3H]WIN 35.428 in the monkey brain. *Synapse* 6:189–195

Chalon S, Emond P, Bodard S, Vilar MP, Thiercelin C, Besnard JC, Guilloteau D (1999) Time course of changes in striatal dopamine transporters and D2 receptors with specific iodinated markers in a rat model of Parkinson's disease. *Synapse* 31:134–139

Delforge J, Loc'h C, Hantraye P, Stulzaft O, Khalili-Varasteh M, Mazière M, Syrota A, Mazière B (1991) Kinetic analysis of central [^{76}Br]bromolisuride binding to dopamine D2 receptors studied by PET. *J Cereb Blood Flow Metab* 11:914–925

Delforge J, Syrota A, Bottlaender M, Varastet M, Loc'h C, Bendriem

B, Crouzel C, Brouillet E, Mazière M (1993) Modeling analysis of [^{11}C]flumazenil kinetics studied by PET: application to a critical study of the equilibrium approaches. *J Cereb Blood Flow Metab* 13:454–468

Delforge J, Spelle L, Bendriem B, Samson Y, Bottlaender M, Papageorgiou S, Syrota A (1996) Quantitation of benzodiazepine receptors in human brain using the partial saturation method. *J Nucl Med* 37:5–11

Delforge J, Bottlaender M, Loc'h C, Guenther I, Fuseau C, Bendriem B, Syrota A, Mazière B (1999) Quantitation of extrastriatal D2 receptors using a very high-affinity ligand (FLB 457) and the multi-injection approach. *J Cereb Blood Flow Metab* 9:533–546

Dollé F, Demphel S, Hinnen F, Fournier D, Vaufrey F, Crouzel C (1998) 6-[^{18}F]Fluoro-L-DOPA by radiofluorodestannylation: a short and simple synthesis of a new labeling precursor. *J Label Cpd Radiopharm* 41:105–114

Dollé F, Bottlaender M, Demphel S, Emond P, Fuseau C, Coulon C, Ottaviani M, Valette H, Loc'h, Halldin C, Mauclaire L, Guilloteau D, Mazière B, Crouzel C (2000) High efficient synthesis of [^{11}C]PE2I, a selective radioligand for the quantification of the dopamine transporter using PET. *J Labelled Cpd Radiopharm* 43:997–1004

Emond P, Garreau L, Chalon S, Boazi M, Caillet M, Bricard J, Frangin Y, Mauclaire L, Besnard JC, Guilloteau D (1997) Synthesis and ligand binding of nortropane derivatives: N-substituted 2beta-carbomethoxy-3beta-(4′-iodophenyl)nortropane and N-(3-iodoprop-(2E)-enyl)-2beta-carbomethoxy-3beta-(3',4′-disubstituted phenyl) nortropane. New high-affinity and selective compounds for the dopamine transporter. *J Med Chem* 40:1366–1372

Frost JJ, Rosier AJ, Reich SG, Smith JS, Ehlers MD, Snyder SH, Ravert HT, Dannals RF (1993) Positron emission tomographic imaging of the dopamine transporter with ^{11}C-WIN 35,428 reveals marked declines in mild Parkinson's disease. *Ann Neurol* 34:423–431

Gaspar P, Febvret A, Colombo J (1993) Serotonergic sprouting in primate MPTP-induced hemiparkinsonism. *Exp Brain Res* 96:100–106

Hantraye P, Brownell AL, Elmaleh D, Spealman RD, Wullner U, Brownell GL, Madras BK, Isacson O (1992) Dopamine fiber detection by [^{11}C]-CFT and PET in a primate model of parkinsonism. *Neuroreport* 3:265–268

Hornykiewicz O (1993) Parkinson's disease and the adaptive capacity of the nigrostriatal dopamine system: possible neurochemical mechanisms. *Adv Neurol* 60:140–147

Hsu SM, Raine L, Fanger H (1981) Use of avidin-biotin-peroxidase complex (ABC) in immunoperoxidase techniques: a comparison between ABC and unlabeled antibody (PAP) procedures. *J Histochem Cytochem* 29:577–580

Ishikawa T, Dhawan V, Kazumata K, Chaly T, Mandel F, Neumeyer J, Margouleff C, Babchyk B, Zanzi I, Eidelberg D (1996) Comparative nigrostriatal dopaminergic imaging with Iodine-123-Beta CIT-FP/SPECT and Fluorine-18–FDOPA/PET. *J Nucl Med* 37:1760–1765

Kaufman MJ, Spealman RD, Madras BK (1991) Distribution of cocaine recognition sites in monkey brain: I. In vitro autoradiography with [3H]CFT. *Synapse* 9:177–187

Kilbourn MR, Sherman PS, Pisani T (1992) Repeated reserpine administration reduces *in vivo* [^{18}F]GBR 13119 binding to the dopamine uptake site. *Eur J Pharmacol* 216:109–112

Kordower JH, Emborg ME, Bloch J, Ma SY, Chu Y, Leventhal L, McBride J, Chen EY, Palfi S, Roitberg BZ, Brown WD, Holden JE, Pyzalski R, Taylor MD, Carvey P, Ling Z, Trono D, Hantraye P, Deglon N, Aebischer P (2000) Neurodegeneration prevented by lentiviral vector delivery of GDNF in primate models of Parkinson's disease. *Science* 290:767–773

Lee CS, Samii A, Sossi V, Ruth TJ, Schulzer M, Holden JE, Wudel J, Pal PK, de la Fuente-Fernandez R, Calne B, Stoessel AJ (2000) *In vivo* positron emission tomographic evidence for compensatory changes in presynaptic dopaminergic nerve terminals in Parkinson's disease. *Ann Neurol* 47:493–502

Lowry OH, Rosebrough NJ, Farr AL, Randall RJ (1951) Protein measurement with the Folin phenol reagent. *J Biol Chem* 193:265–275

Maes F, Collignon A, Vandermeulen D, Marchal G, Suetens P (1997) Multimodality image registration by maximization of mutual information. *IEEE Trans Med Imaging* 16:187–98

Morris ED, Babich JW, Alpert NM, Bonab AA, Livni E, Weise S, Hsu H, Christian BT, Madras BK, Fischman AJ (1996) Quantification of dopamine transporter density in monkeys by dynamic PET imaging of multiple injections of ^{11}C-CFT. *Synapse* 24:262–272

Namavari M, Bishop A, Satyamurthy N, Bida G, Barrio JR (1992) Regioselective radiofluorodestannylation with [^{18}F]F_2 and [^{18}F]CH_3COOF: a high yield synthesis of 6-[^{18}F]Fluoro-L-DOPA. *Appl Radiat Isot* 43:989–996

Neumeyer JL, Wang S, Gao Y, Milius RA, Kula NS, Campbell A, Baldessarini RJ, Zea-Ponce Y, Baldwin RM, Innis RB (1994) N-ω-fluoroalkyl analogs of (1R)-2 β-carbomethoxy-3 β-(4-iodophenyl)-tropane (β-CIT): radiotracers for positron emission tomography and single photon emission computed tomography imaging of dopamine transporters. *J Med Chem* 37:1558–1561

Nurmi E, Ruottinen HM, Kaasinen V, Bergman J, Haaparanta M, Solin O, Rinne JO (2000) Progression in Parkinson's disease: a positron emission tomography study with a dopamine transporter ligand [^{18}F]CFT. *Ann Neurol* 47:804–808

Pate BD, Kawamata T, Yamada T, Mc Geer EG, Hewitt KA, Snow BJ, Ruth TJ, Calne DB (1993) Correlation of striatal fluorodopa uptake in the MPTP monkey with dopaminergic indices. *Ann Neurol* 34:331–338

Patlak CK, Blasberg RG (1985) Graphical evaluation of blood-to-brain transfer constants multiple-time uptake data. Generalizations. *J Cereb Blood Flow Metab* 5:584–590

Pietrzyk U, Herholz K, Fink G, Jacobs A, Mielke R, Slansky I, Wurker M, Heiss WD (1994) An interactive technique for three-dimensional image registration: validation for PET, SPECT, MRI and CT brain studies. *J Nucl Med* 35:2011–2018

Rakshi JS, Uema T, Ito K, Bailey DL, Morrish PK, Ashburner J, Dagher A, Jenkins IH, Friston KJ, Brooks DJ (1999) Frontal, mid- brain and striatal dopaminergic function in early and advanced Parkinson's disease. A 3D [(18)F]dopa-PET study. *Brain* 122:1637–1650

Remy P, Samson Y, Hantraye P, Fontaine A, Defer G, Mangin JF, Fenelon G, Geny C, Ricolfi F, Frouin V, N'Guyen JP, Jeny R, Degos JD, Peschanski M, Cesaro P (1995) Clinical correlates of [^{18}F]fluorodopa uptake in five grafted parkinsonian patients. *Ann Neurol* 38:580–588

Ribeiro MJ, Vidailhet M, Loc'h C, Samson Y, Dupel C, Cesaro P, NGuyen JP, Hantraye P, Remy P (2000) Comparison of dopaminergic function and dopamine transporter density at different stages of Parkinson's disease: a PET study. *Neurology* 54:A113

Snow BJ, Tooyama I, McGeer EG, Yamada T, Calne DB, Takahashi H, Kimura H (1993) Human positron emission tomographic [^{18}F]fluorodopa studies correlate with dopamine cell counts and levels. *Ann Neurol* 34:324–330

Song DD, Haber SN (2000) Striatal responses to partial dopaminergic lesion: evidence for compensatory sprouting. *J Neurosci* 20:5102–5114

Varastet M, Hantraye P, Bottlaender M, Fuseau C, Cesaro P, Brouillet E, Schmid L, Hinnen F, Mazière M (1993) Progressive biphasic damage to the nigrostriatal pathway induced by chronic MPTP treatment in baboons: a positron emission tomography study using 6- (^{18}F) fluoro-L Dopa. *Curr Topics Pharmacol* 2:11–19

Vilpoux C, Leroux-Nicollet I, Naudon L, Raisman-Vozari R, Costentin J (2000) Reserpine or chronic paroxetine treatments do not modify the vesicular monoamine transporter 2 expression in serotonin-containing regions of the rat brain. *Neuropharmacology* 39:1075–1082

Watson CC, Newport D, Casey ME, et al (1997) Evaluation of simulation-based scatter correction for 3D PETR cardiac imaging. *IEEE Trans Nucl Sci* 44:90–97

West MJ, Slomianka L, Gundersen HJG (1991) Unbiased stereological estimation of the total number of neurons in the subdivisions of the rat hippocampus using the optical fractionator. *Anat Rec* 231:482–497

West MJ, Oestergaard K, Andreasen OA, Finsen B (1996) Estimation of the number of somatostatin neurons in the striatum: an *in situ* hybridization study using the optical fractionator method. *J Comp Neurol* 370:11–22

Zigmond MJ, Abercrombie ED, Berger TW, Grace AA, Stricker EM (1990) Compensations after lesions of central dopaminergic neurons: some clinical and basic implications. *Trends Neurosci* 13:290–296